

Two dimensional EBG structures for multiband noise mitigation

Antonio Ciccomancini SCOGNA¹, Antonio ORLANDI²

¹ CST of America, 492 Old Connecticut path, suite505, Framingham, MA, 01701, USA
e-mail: antonio.ciccomancini@cst.com

² UAq EMC Lab, University of L'Aquila, 67100, Poggio di Roio, L'Aquila-ITALY
e-mail: orlandi@ing.univaq.it

Abstract

In this paper a two dimensional (2D) electromagnetic Bandgap (EBG) structure is proposed for multi band noise mitigation in PWR/GND plane pairs. Excellent noise suppression (-60 dB) is achieved in multiple bands within the range 0–8 GHz with a low start frequency. Because of the 2D EBG, no additional metal layer is required. Signal Integrity analysis is also studied by modelling a microstrip to stripline transition (both single ended and differential) and by evaluating insertion loss, TDR as well as eye diagram.

1. Introduction

Simultaneous switching noise (SSN) on the power/ground (PWR/GND) buses is one of the major concerns for the design of high speed communication systems with faster edge rates, higher integration and at the same time lower voltage level. It is well known that SSN is generated by the propagation of unwanted modes in PWR/GND layers which act as cavity guiding those modes. Cavity resonance suppression in multilayer printed circuit boards (PCBs) by means of electromagnetic bandgap structures (EBGs) was recently introduced [1]. Later, the same concept has been also applied to reduce electromagnetic interference (EMI) [2]. Since then design guidelines either based on direct methods or indirect methods have been explored in multiple papers [3–6]. Nevertheless most of the works are focused on how to extend the stop band for more efficient noise suppression (in high frequency) as well as on how to lower the effective frequency ranges of the EBGs. Not many papers are available in the literature focusing on the signal integrity (SI) of high speed interconnects and power delivery network (PDN) in multilayer PCB which are very important for a successful application of EBGs [7]. Due to the patterned EBG layer the return current path can produce multiple impedance variation (clearly observed in the TDR waveform), consistent signal distortion (time signal analysis) as well as degradation (insertion loss and eye diagram).

In the present paper two different aspects are analysed: (1) the extension of the stop band by designing an EBG which produce multiple bands of noise attenuation; (2) the SI of the proposed design by studying a

simple microstrip to stripline transition in time and frequency domain. The proposed 2D EBG consists of an improved meander line with square metal patches; vias are not required which means lower cost process, since the proposed EBG layer can be designed and fabricated by using any standard PCB process. Due to the periodic inductor and capacitor (LC) network realized by the combining effect of the solid GND and the EBG PWR plane, multiple stop bands can be achieved. The structure of the paper is the following: in the next section the two dimensional (2D) EBG is illustrated and the noise coefficient is numerically calculated by considering multiple points on a generic PCB. In section III the SI of a microstrip to stripline transition is analysed as a possible worst case and both time and frequency domain results are provided. Finally section IV, we draw some concluding remarks.

2. Proposed EBG structure and analysis of noise attenuation

The shape of the considered EBG is illustrated along with the relevant dimensions in Figure1: it is a 2D square patch with meander lines.

The simulated test board is a 2 layers PWR/GND layers board whose dimensions are $W = 9.6$ cm, $H = 7.2$ cm, $h = 0.02$ cm. The dielectric material is FR4 ($\epsilon_r = 4.4$ and $\tan \delta = 0.02$ at 0.5 GHz). The metal is Copper (Cu) whose thickness is 17 μ m.

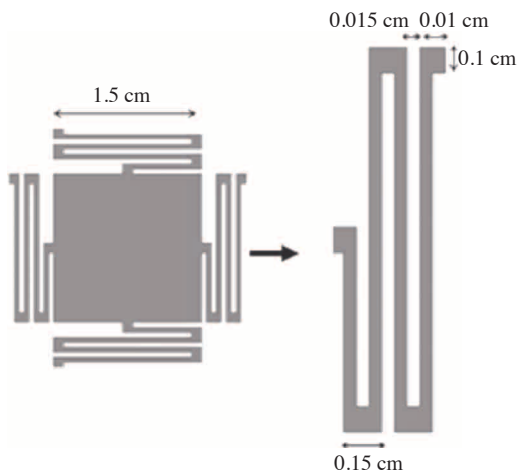


Figure 1. Metal patch of the considered EBG.

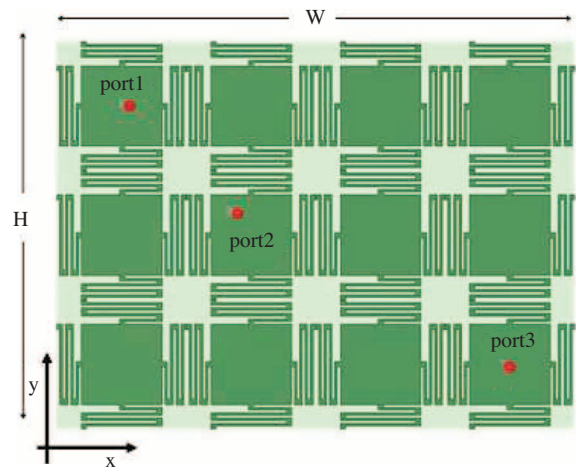


Figure 2. Top view of the considered PWR/GND plane pairs with EBG structure.

A Finite Integration Technique (FIT) based numerical code [8] is used for the numerical simulations. In order to validate the code, time (TD) and frequency (FD) domain solvers are both used to calculate the noise coefficients (S_{21} and S_{31}) for the configuration illustrated in Figure 2. The calculations are performed on a dual core Pentium with 2 GB of RAM and the simulation time is approximately 30 min per port. The excitation of the system is given by a lumped source placed in position $x=1$, $y=6$ cm. Results are reported in Figure 3 and good agreement can be observed over the all considered frequency range 0–8 GHz.

Each figure also reports the FSV Grade-Spread chart as indicated by the IEEE Standard for data comparison [9]: the presence of the FSV figures of merits in the red and yellow areas indicates a high quality of the comparison for the data.

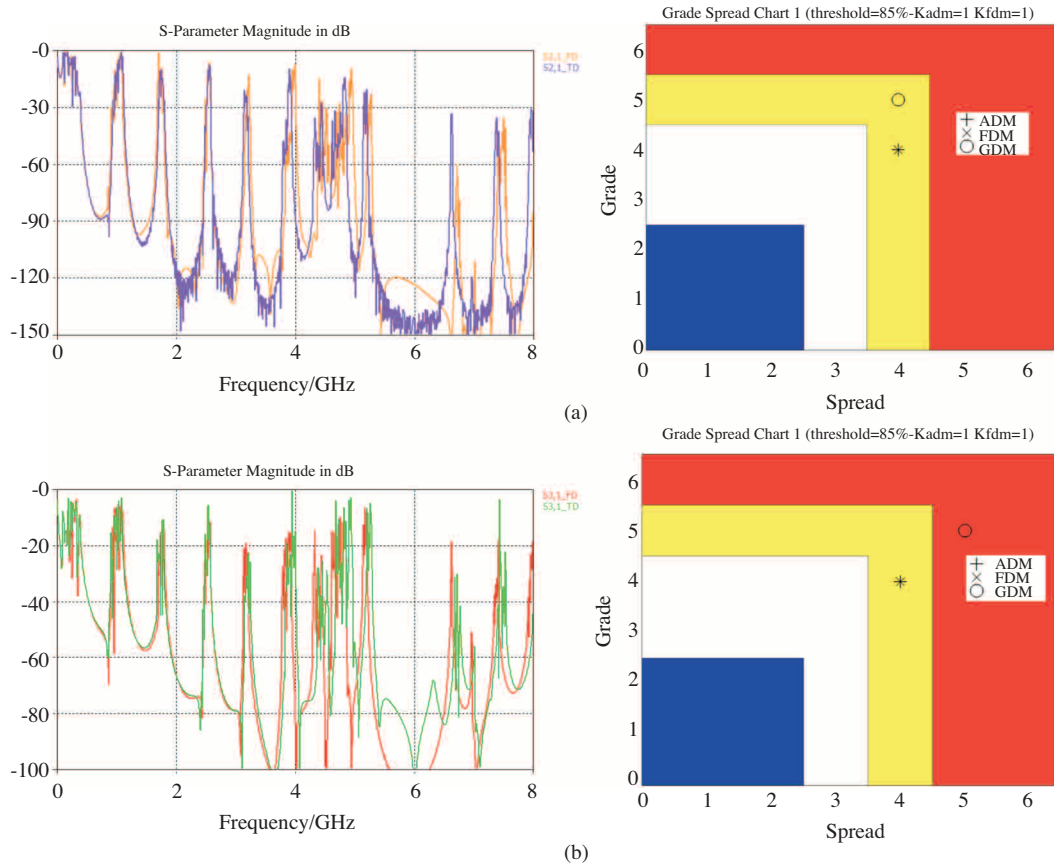


Figure 3. Noise coefficients (a) $|S_{21}|$ and (b) $|S_{31}|$.

Looking at the results it is also possible to see consistent multi band noise suppression in the considered frequency range (0.2–1 GHz, 1.1–1.8 GHz, 1.9–2.3 GHz...). With the exception of few very sharp and defined resonances excellent noise suppression is achieved. Furthermore noise attenuation is also achieved in the low frequency range. Figure 4 illustrates the noise coefficient on ports 2 and 3 for the proposed EBG geometry; the comparison with the reference board with continuous PWR/GND planes is also illustrated and it is possible to see consistent noise mitigation within the considered frequency range 0–8 GHz. A further confirmation of the previous observations also comes from the plot of the magnetic field distribution at 3.5 GHz, a frequency value within the stop band of the proposed EBG (see Figure 5).

Isolation is of course desirable between the input Port 1 and the output Ports 2 and 3. It is important to note that the noise generated by the current source on the input port can not propagate to the other metal patches characterizing the EBG structure (Figure 5(b)), which means that eventual noise generated by digital circuits cannot propagate to the RF circuits located at port 2 and/or port 3 (output ports).

Dispersion diagrams can be also extracted for the considered EBG structure by considering only one patch (or a unit cell) and applying a periodic boundary condition on the sides of the cell (to mimic the presence of the cell in a periodic structure extending to infinity), and Perfect Electric Conductor (PEC) boundary condition on the top and bottom of the cell for the power planes (these boundary conditions do not impact the results that are depending on the periodicity of the structure).

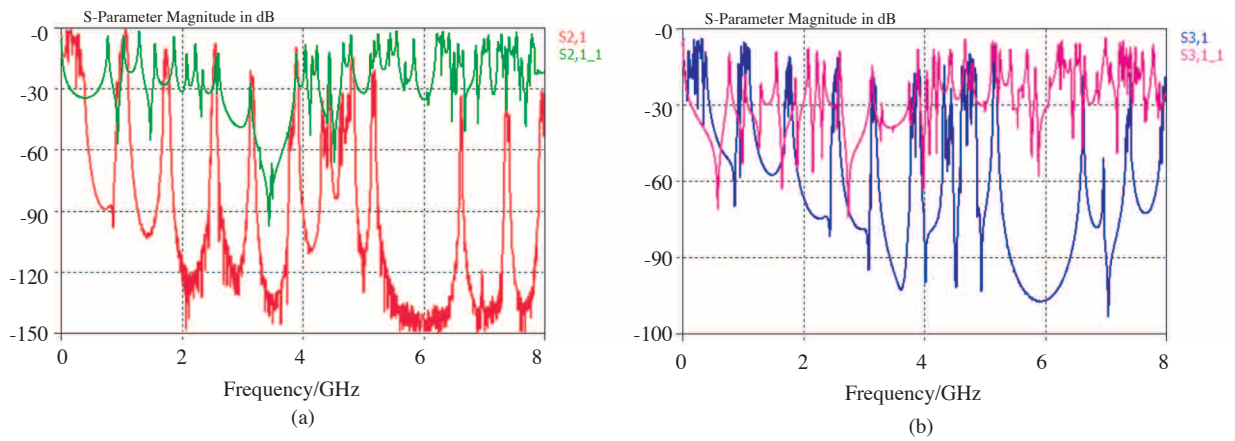


Figure 4. Noise coefficients: (a) $|S_{21}|$ and (b) $|S_{31}|$: comparison between continuous reference plane ($S_{21,1}$ and $S_{31,1}$) and EBG layer (S_{21} and S_{31}).

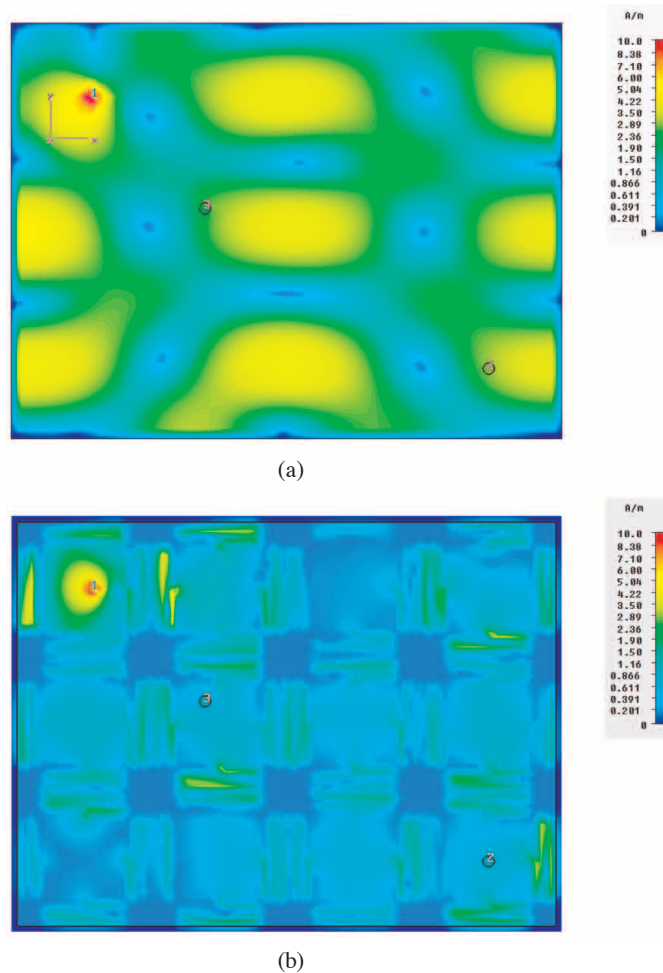


Figure 5. Magnetic field distribution at 3.5 GHz, within the stop band, for (a) continuous reference plane, (b) EBG layer.

These diagrams present propagating modes and band gaps that can potentially exist between such modes (in a periodic structure at a given frequency of operation, many modes in different directions may be excited). Figure 6 shows the dispersion diagram related to the unit cell proposed in Figure 1 according to the Brillouin theory: multiple stop bands are clearly visible in the considered frequency range, in particular we have 200 MHz–0.9 GHz, 1 GHz–1.7 GHz, 2.4 GHz–3.2 GHz and 3.8 GHz–4.4 GHz.

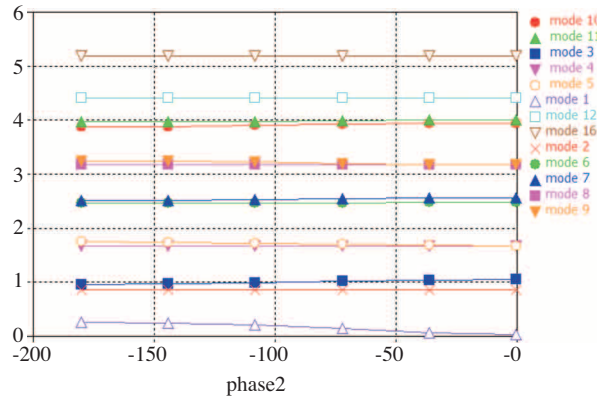


Figure 6. Dispersion diagram for the EBG structure (calculated modes 1–11).

3. Signal Integrity analysis

Although the proposed PWR/GND plane design shows excellent performance on eliminating SSN noise at broad band frequency ranges, the presence of the EBG structure might degrade the quality of signals propagating on traces.

For this reason a microstrip to stripline transition is modelled in order to study the SI performance in presence of the EBG structure. The considered structure is depicted in Figure 7(a, b) where the top view of the board and the cross section (stack-up) are illustrated. In particular two different configurations of lines (trace thickness $t_{Cu} = 17 \mu\text{m}$) are investigated: single ended (SE, characteristic impedance $Z_c = 50 \Omega$) and differential (DIFF, $Z_c = 100 \Omega$).

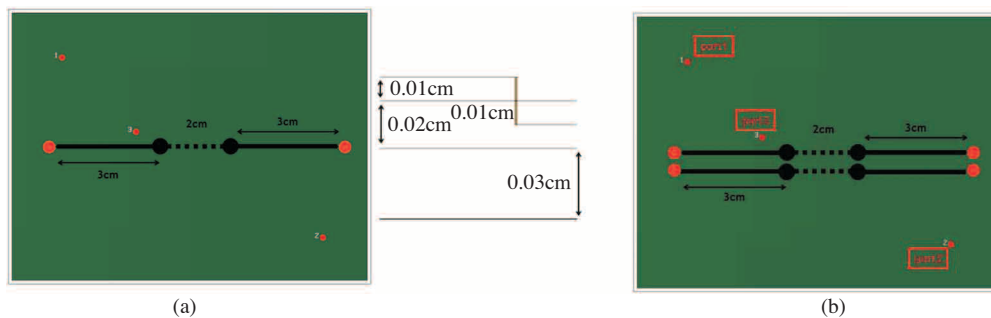


Figure 7. a): SE and b): DIFF microstrip to stripline transition.

Figure 8 compares the insertion loss for the structure with EGB layer and continuous reference plane. In the low frequency range (up to 2 GHz) the curves are almost the same, but for higher frequencies a shift

in the resonances is observed, even though the shape is overall very similar with the exception of two deeper resonances at 4.9 GHz and 7.8 GHz.

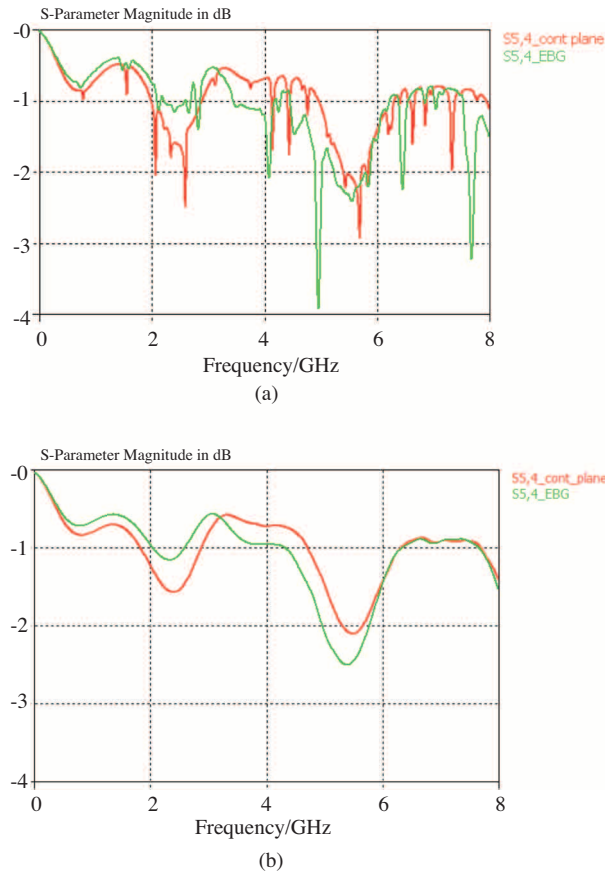


Figure 8. Insertion loss for (a) SE and (b) DIFF signalling of microstrip to stripline transition.

However, the DIFF signalling allows to consistently mitigating those resonances and the performance of the considered transmission line is fully comparable to the case of DIFF signalling over continuous reference plane (see Figure 8b). By considering a figure of merit of -3 dB within the considered, frequency range the SE transition in presence of EBG allow to approximately utilize 5.5 GHz of bandwidth, while when the DIFF signalling is used the useful bandwidth is the whole frequency range 0–10 GHz. The TDR is also calculated and the results are reported in Figure 9.

Although the presence of the patterned EBG metal layer should cause multiple impedance variation, in this case the deviation is very small and an even lower impedance variation is observed in the range 0–1 ns due to the extra inductive behaviour which reduces the capacitive bump of the continuous PWR/GND plane pair.

This is probably due to the fact that the dimension of the single patch is still consistent compared to the electric wavelength, therefore the current return path is still relatively continuous and not broken by multiple/consecutive gaps.

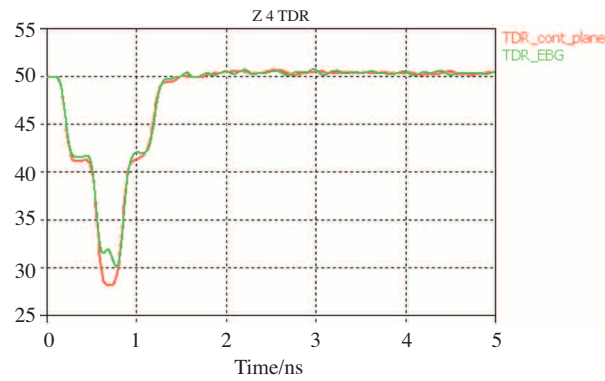


Figure 9. SE TDR: comparison between continuous reference plane and EBG layer.

Furthermore eye diagrams are calculated for the previous structure. The eye patterns (EP) at the output port of the transmission line are computed from the computation of the S-parameters in frequency domain. A pseudorandom (PRBS) bit sequence with the following parameters $T_{bit} = 0.3$ ns, $t_r = t_f = 0.01$ ns, $V_{high} = 1$ V, $V_{low} = 0$ V is used as input. Two parameters, Maximum Eye Opening (MEO) and Maximum Eye Width (MEW) are used as metrics of the eye pattern quality.

For the reference board with continuous reference plane it results MEO=0.82 V and MEW=0.31 ns (see Figure 10(a)) and for the board with EBG structure, MEO=0.8 V and MEW=0.3 ns (see Figure 10(b)).

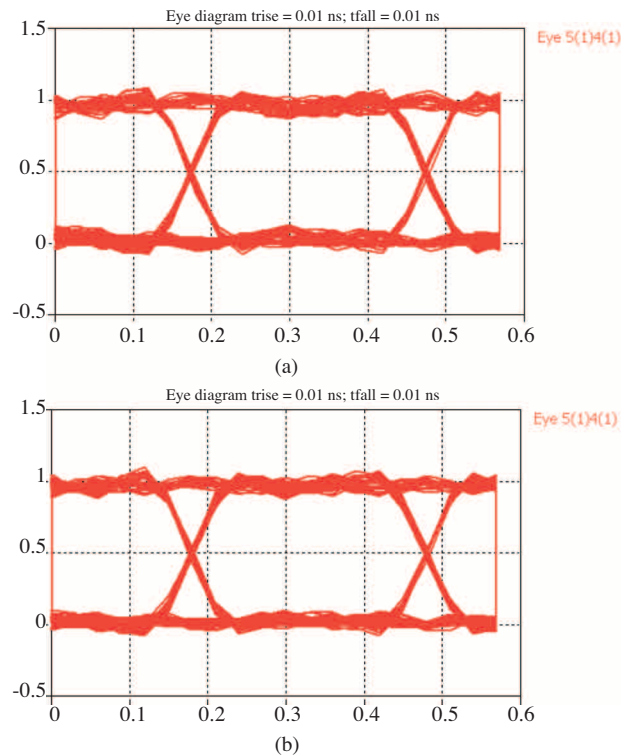


Figure 10. Eye diagram: comparison between (a) continuous reference plane and (b) EBG layer.

The performances of the EBG structures should also be evaluated in terms of their ability to reduce the electromagnetic noise generated between the planes by the currents flowing in the lines and in particular through the vertical vias fully or partially crossing the planes. The results at ports 1, 2 and 3 when port 4 (input for the transmission line) is excited are illustrated in Figure 11. Good noise suppression is observed for the all frequency range even for the port 3 which is very close to the considered signal line.

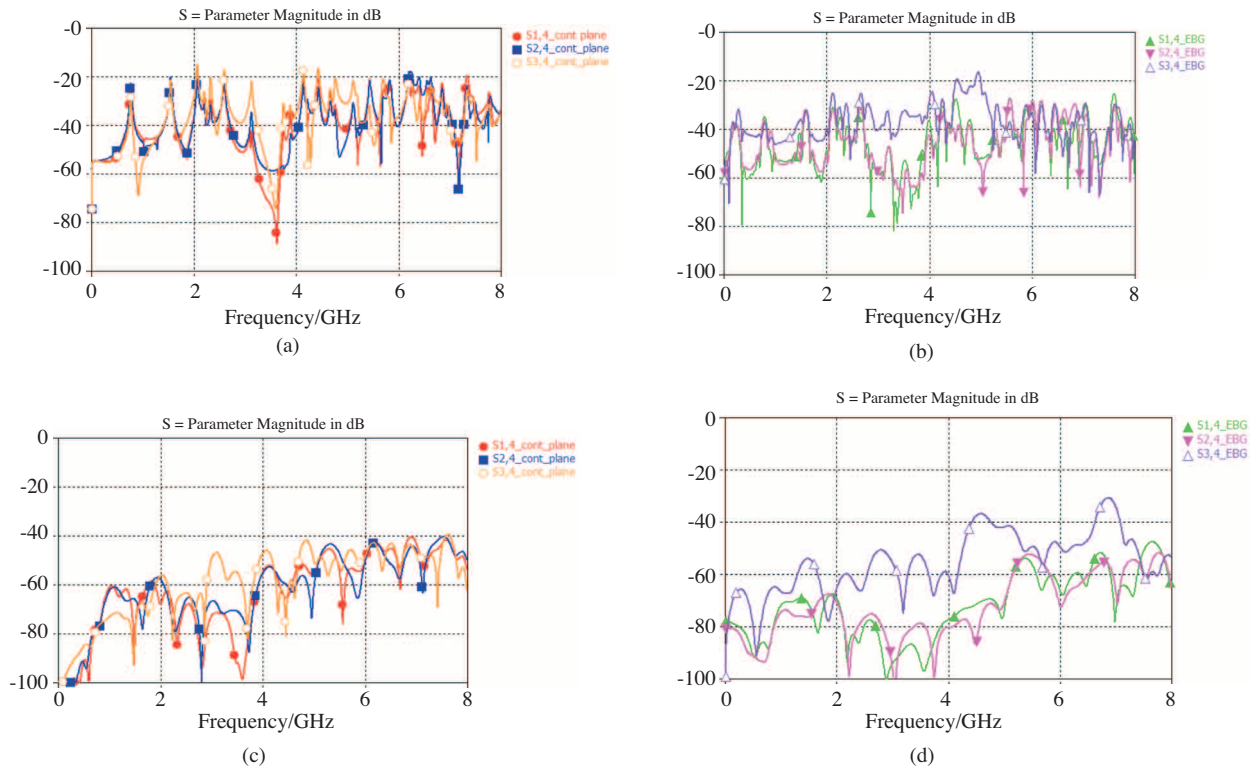


Figure 11. Noise coefficient between input and output ports ($|S_{14}|$, $|S_{24}|$ and $|S_{31}|$): comparison between (a–b) SE; and (c–d) DIFF signalling.

4. Conclusions

In this paper multi band noise mitigation by means of a 2D EBG with square patches and meander lines has been presented. The calculated noise coefficient reveals excellent noise suppression in the frequency range 0–8 GHz. The signal integrity analysis is investigated by considering a microstrip to stripline transition. Time and frequency domain results are provided (insertion loss, TDR and eye diagram) which prove the effectiveness of the proposed design due to very small impedance variation and same performance in terms of quality of transmitted signal (insertion loss and eye diagram).

References

- [1] R. Abhari, G.V. Eleftheriades, “Metallo - dielectric electromagnetic band gap structures for suppression and isolation of parallel-plate noise in high speed circuits”, *IEEE Trans. On Microwave Theory and Tech*, vol. 51, no. 6, pp. 1629–1639, June 2003.

- [2] S. Shahparnia, O. M. Ramahi, "Electromagnetic interference (EMI) and reduction from printed circuit boards (PCB) using electromagnetic bandgap structures", *IEEE Trans. Electromagnetic Comp*, vol. 46, no. 4, pp. 580–587, November 2004.
- [3] X.H. Wang, B.Z.Wang, Ye-Hai Bi, "A novel uniplanar compact photonic Bandgap power plane with ultra-broadband suppression of ground bounce noise", *IEEE Trans. Microwave and Wireless Components Letters*, vol. 16, no. 5, pp. 267–268, May 2006.
- [4] J. Qin and O. M. Ramahi, "Ultra-Wideband Mitigation of Simultaneous Switching Noise Using Novel Planar Electromagnetic Bandgap Structures", *IEEE Microwave and Wireless Components Letters*, Vol. 16, No. 9, pp. 487–489, September 2006.
- [5] A. Ciccomancini Scogna, "Noise suppression in high speed digital circuits by means of a novel EBG structure with triangle patches and hexagonal arrays", *IEEE Int. Symp. on EMC*, Hawaii, July 2007.
- [6] A. Ciccomancini Scogna, M. Schauer, "A Novel Electromagnetic Bandgap Structure for SSN Suppression in PWR/GND plane pairs", in *Proc. of ECTC 07*, Reno, Nevada.
- [7] A. Ciccomancini Scogna, A. Orlandi, V. Ricchiuti, "Signal Integrity Analysis of Single-Ended and Differential Signaling in PCBs with EBG structure", *IEEE Int. Symp. on EMC*, Detroit, August 2008
- [8] CST STUDIO SUITETM 2008, www.cst.com
- [9] IEEE Standard P1597, Standard for Validation of Computational Electromagnetics Computer modelling and Simulation, Part 1-2, September 2008.